

Quantum manipulation via atomic-scale magnetoelectric effects

Anh T. Ngo,¹ Javier Rodriguez-Laguna,² Sergio E. Ulloa,¹ and Eugene H. Kim^{3,4}

¹*Department of Physics, and Nanoscale and Quantum Phenomena Institute, Ohio University, 45701 USA*

²*ICFO-Institut de Ciències Fotoniques, Barcelona, Spain*

³*Instituto de Física Teórica, UAM-CSIC, Madrid 28049, Spain*

⁴*Department of Physics, University of Windsor, Windsor, Ontario, Canada N9B 3P4*

Magnetoelectric effects at the atomic scale are demonstrated to afford unique functionality. This is shown explicitly for a quantum corral defined by a wall of magnetic atoms deposited on a metal surface where spin-orbit coupling is observable. We show these magnetoelectric effects allow one to control the properties of the systems placed inside the corral as well as their electronic signatures; they provide alternative tools for probing electronic properties at the atomic scale.

It has long been appreciated that interesting and unique properties arise from the coupling between the charge and magnetic degrees of freedom in materials. Advances in our understanding of the physics regulating these properties have given rise to systems with a number of practical applications. Prominent examples include multiferroic materials, which exhibit simultaneous and cooperative ferroelectric and magnetic ordering,¹ as well as giant² and colossal³ magnetoresistance materials, which exhibit substantial changes in their electronic transport with the application of small magnetic fields. These and other *magnetoelectric* (ME) *effects* — coupling charge and magnetic degrees of freedom — provide unique functionalities and hold promise for novel device applications.⁴

With the continuing drive to miniaturize electronic devices, there is interest in better controlling or/and enhancing the functionality of nanoscale systems; there is particular interest in novel devices that utilize phenomena inherent/unique to these nanometer scales.⁵ Here, we predict unique functionality in a nanoscale device arising from the coupling of charge and magnetic degrees of freedom in the ultimate miniaturization, namely where devices are built atom-by-atom.^{5,6} We demonstrate that the interplay of spin-orbit coupling and electronic scattering results in ME effects which enable exquisite control at the atomic scale. This control provides a powerful tool for manipulating the response of quantum systems, adding desirable functionalities not only for fundamental studies, but also for possible future devices built in a “bottom up” approach.

Our device system consists of a quantum corral (QC) on a metal surface with spin-orbit coupling (SOC) (e.g. Au(111)⁷), where the QC’s wall is made of magnetic atoms. We demonstrate the possibility of controlling the electronic properties of the QC by changing the magnetization of the atoms forming the QC’s wall; we show that these ME effects allow one to control the properties of systems placed inside the QC as well as their electronic signatures. This control provides powerful alternative tools for probing and manipulating electronic properties at the atomic scale.

The Hamiltonian for the system has the form $\hat{H}=\hat{H}_{\text{QC}}+\hat{H}_1$, where \hat{H}_{QC} describes the QC, and \hat{H}_1 describes a system we place inside the QC, whose properties will be controlled and/or probed (see below). We

describe the QC by the Hamiltonian $\hat{H}_{\text{QC}}=\hat{H}_0+\hat{V}$, where \hat{H}_0 describes a two-dimensional electron gas (2DEG) with SOC, and \hat{V} is a scattering potential describing the QC’s wall. The Hamiltonian for the 2DEG is

$$\hat{H}_0 = \frac{1}{2m^*} \mathbf{p}^2 + \lambda \hat{z} \cdot (\mathbf{p} \times \vec{\sigma}) \quad (1)$$

where \mathbf{p} is the momentum operator of the 2DEG, $\{\sigma^\mu\}$ are the Pauli matrices, m^* is the electron’s band mass, and λ parameterizes the SOC. As described above, we are interested in the case where the QC’s wall is made of magnetic atoms — being interested in the system’s low-energy properties, we treat the atoms as a collection of *s*-wave scatterers;⁸ we take

$$\hat{V} = \sum_i \left(V_0 + \frac{J}{2} \vec{\tau}_i \cdot \vec{\sigma} \right) \delta(\mathbf{r} - \mathbf{r}_i), \quad (2)$$

where \mathbf{r} is the position operator of the 2DEG, V_0 describes the potential scattering, J is the exchange coupling between the (magnetic) atoms and the 2DEG, $\vec{\tau}_i$ is the spin operator of the i^{th} atom, and the atoms are located at the positions $\{\mathbf{r}_i\}$.⁹ The form(s) of H_1 will be specified subsequently.

In this work, we will be interested in the case where the atoms of the QC’s wall are ferromagnetically (FM) ordered — we assume the atoms’ moments are sufficiently large and treat them as classical variables: $(J/2)\langle\vec{\tau}_i\rangle=\mathbf{M}$. The physical quantity of interest is the electronic local density of states (LDOS) in the QC, $A(\mathbf{r}, \omega)$. [The differential conductance measured in scanning tunneling microscopy is proportional to $A(\mathbf{r}, \omega)$.¹⁰] This is obtained from the QC’s retarded Green’s function (GF) $G(\mathbf{r}, \mathbf{r}'; \omega)$ via

$$A(\mathbf{r}, \omega) = -\frac{1}{\pi} \text{Im} \{ \text{Tr}[G(\mathbf{r}, \mathbf{r}; \omega)] \}, \quad (3)$$

where^{10,11}

$$G(\mathbf{r}, \mathbf{r}'; \omega) = G_0(\mathbf{r}, \mathbf{r}'; \omega) + G_0(\mathbf{r}, \mathbf{R}_0; \omega) \hat{T}(\omega) G_0(\mathbf{R}_0, \mathbf{r}'; \omega). \quad (4)$$

In Eq. 4, the T -matrix $\hat{T}(\omega)$ describes the influence of H_1 . Furthermore, $G_0(\mathbf{r}, \mathbf{r}'; \omega)$ is the bare GF of the QC, i.e. the GF in the absence of \hat{H}_1 .⁹

In what follows, we choose $(\pi\rho_0)V_0=0.3$ and $(\pi\rho_0)|\mathbf{M}|=0.5$ ($\rho_0=m^*/2\pi$);⁹ we consider physically reasonable values of the parameters for the 2DEG:¹² a Fermi energy $E_F=0.5\text{eV}$, $m^*=0.26m_e$ (m_e is the bare electron mass), and $\lambda=4\times 10^{-11}\text{eV}\cdot\text{m}$. The results we show are for an elliptical QC with 40 atoms, similar to what has been realized experimentally:¹³ $(x/a)^2+(y/b)^2=R^2$ with $R=57.22\text{\AA}$, $a/b=1.5$, and $(\pm c,0)=(\pm\sqrt{a^2-b^2},0)$ being the ellipse's foci; we will also comment about results obtained for a circular QC. It should be stressed the results we report are robust — changes in the relative size and phase of the ratio \mathbf{M}/V_0 have only quantitative effects on the results, leaving our overall discussion and conclusions unaffected; furthermore, the corral's geometry can, in fact, be tuned to enhance/optimize the ME effects (depending on the parameters).

We begin by discussing the electronic properties of the QC (with $\hat{H}_1=0$). Fig. 1 shows a spatial scan of the LDOS at E_F for different directions of \mathbf{M} . Notice how the LDOS changes as one changes the direction of \mathbf{M} — the magnetization of the QC's wall and the SOC give rise to strong ME effects at the atomic scale. These effects are due to the breaking of SU(2) spin-rotation invariance by the SOC. Furthermore, the differences in the LDOS for $\mathbf{M}=|\mathbf{M}|\hat{x}$ and $\mathbf{M}=|\mathbf{M}|\hat{y}$ in the elliptical QC are due to the breaking of rotational invariance — for a circular QC, the DOS for $\mathbf{M}=|\mathbf{M}|\hat{x}$ and $\mathbf{M}=|\mathbf{M}|\hat{y}$ are identical. Fig. 2 shows the energy dependence of the DOS at particular points in the QC — changing the direction of \mathbf{M} changes the energy dependence of the DOS; indeed, by carefully choosing the position in the QC, the changes can be quite pronounced [see Fig. 2(b)]. For reference, the DOS with $|\mathbf{M}|=0$ is also shown, as well as the DOS with $\lambda=0$ (in the inset).

The ME effects exhibited by this system could find utility in a variety of applications that exploit the spatial and/or energy dependence of the QC's LDOS. To illustrate the utility of the spatial dependence of the LDOS, we place a spin-1/2 magnetic impurity at a position \mathbf{R}_0

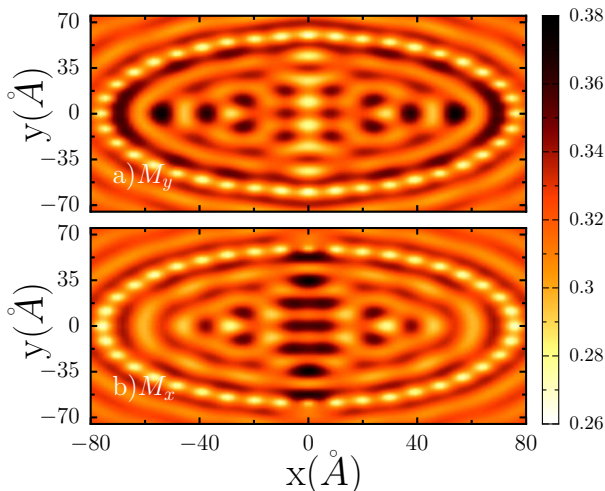


FIG. 1: Spatial scan of the LDOS at E_F : (a) $\mathbf{M}=|\mathbf{M}|\hat{y}$ (b) $\mathbf{M}=|\mathbf{M}|\hat{x}$.

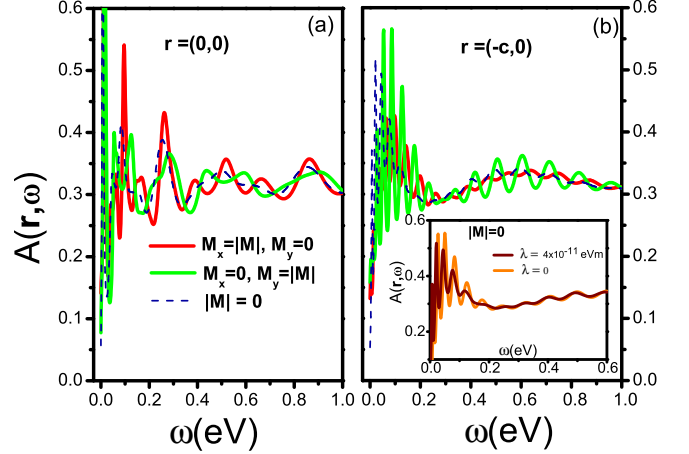


FIG. 2: Energy dependence of the LDOS for different \mathbf{M} : (a) $\mathbf{r}=(0,0)$ (b) $\mathbf{r}=(-c,0)$. Inset: LDOS at $(-c,0)$ for $|\mathbf{M}|=0$ with and without SOC.

inside the QC; we investigate how its low-energy properties depend on its position. We describe the magnetic impurity by the Hamiltonian

$$\hat{H}_1 = J_K \bar{\tau} \cdot \mathbf{S}(\mathbf{R}_0), \quad (5)$$

where $\bar{\tau}$ is the impurity's spin operator, $\mathbf{S}(\mathbf{R}_0)$ is the 2DEG's spin operator at the position \mathbf{R}_0 , and J_K is the exchange coupling between the impurity spin and the 2DEG. In what follows, we take $J_K > 0$.⁹

Interestingly, this seemingly simple system exhibits nontrivial behavior in the infrared, due to quantum fluctuations — a strongly correlated state arises, where a cloud of conduction electrons forms a singlet with the impurity.¹¹ This strongly correlated state manifests itself via a resonance at (or near) the Fermi energy, referred to as the Kondo resonance (KR). This can be seen in Fig. 3, where the imaginary part of the impurity's T -matrix is

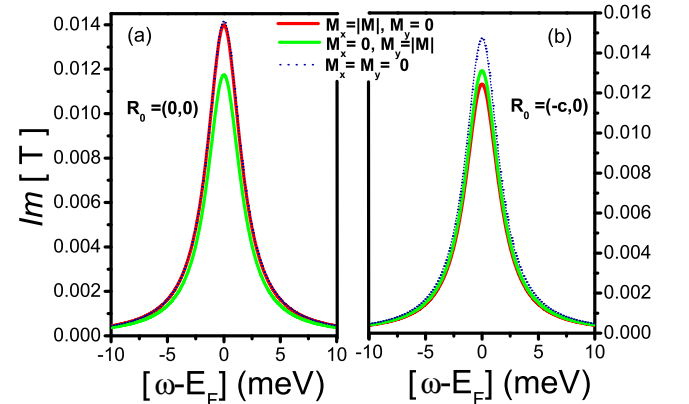


FIG. 3: Imaginary part of the T -matrix due to a magnetic impurity for different \mathbf{M} : (a) impurity at the origin $\mathbf{R}_0=(0,0)$ (b) impurity at the focus $\mathbf{R}_0=(-c,0)$.

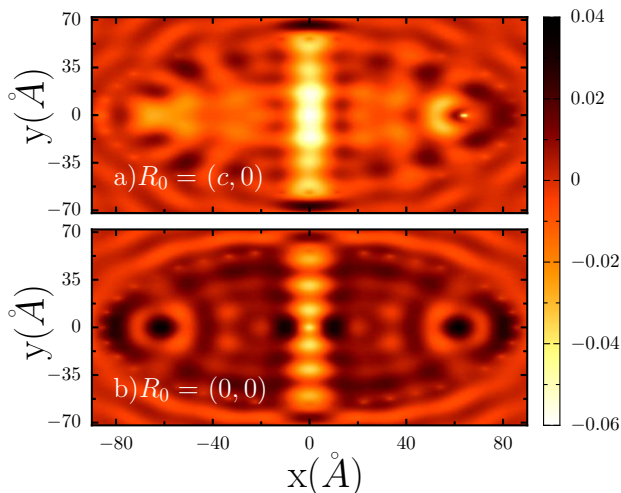


FIG. 4: Spatial dependence of the LDOS difference at E_F due to a magnetic impurity, $\delta A(\mathbf{r}, E_F)$ (see text): (a) impurity at the focus $\mathbf{R}_0=(c, 0)$ (b) impurity at the origin $\mathbf{R}_0=(0, 0)$.

shown and, in particular, the KR appears. Furthermore, the width of this KR represents the dynamically generated scale characteristic of this strongly correlated state, the Kondo temperature T_K .¹¹

The ME effects allow one to control the Kondo effect exhibited by the magnetic impurity in the QC; more generally, it allows one to control the magnetic properties of an atom placed in the QC. Indeed, Fig. 3 shows that the KR can be controlled by changing (the direction of) \mathbf{M} . Furthermore, we see that the change in the KR depends on the position at which the impurity is placed¹⁴ — one can control the impurity's properties in a desired way by a judicious choice of its position. It should also be noted that, besides impacting the properties of the magnetic impurity, the QC is also impacted by the magnetic impurity; the impurity's influence on the QC depends on its position. This can be seen in Fig. 4, where a spatial scan of the quantity $\delta A(\mathbf{r}, E_F) = A(\mathbf{r}, E_F)_{\hat{x}} - A(\mathbf{r}, E_F)_{\hat{y}}$ — the difference in the LDOS (at E_F) between $\mathbf{M} = |\mathbf{M}|\hat{x}$ and $\mathbf{M} = |\mathbf{M}|\hat{y}$ — is shown for different positions of the magnetic impurity. [Results obtained for a circular QC are qualitatively similar to those obtained for an elliptical QC.]

As we saw above, the ME effects allow manipulation of both the spatial and energy dependence of the QC's LDOS. As we now demonstrate, this change in the energy dependence of the DOS can be used for signal filtering. To this end, we place a molecule in the QC at the focus $(c, 0)$, such that a vibrational mode (VM) of this molecule couples to the 2DEG of the QC; we investigate the image or "mirage" of the VM at the other focus $(-c, 0)$. We describe the VM by¹⁵

$$\hat{H}_1 = \frac{1}{2}p^2 + \frac{1}{2}\Omega^2 x^2 + g x n(\mathbf{R}_0), \quad (6)$$

where x (p) is the position (momentum) operator of the VM, Ω is its characteristic frequency, $n(\mathbf{R}_0)$ is the 2DEG's density operator at the position $\mathbf{R}_0=(c, 0)$, and g describes the coupling between the VM and the 2DEG. In

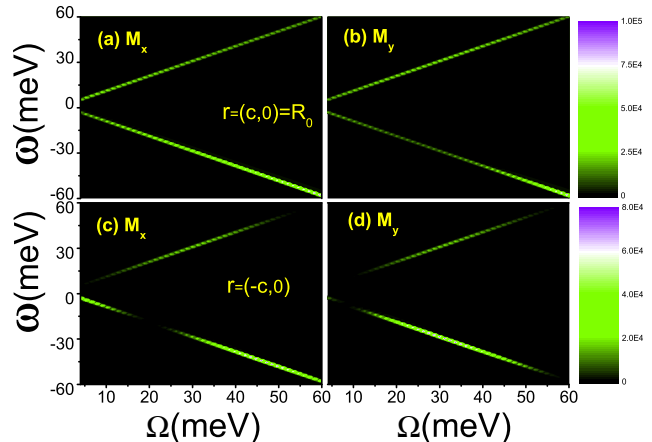


FIG. 5: Maps of $|\partial_\omega \delta A(\mathbf{r}; \omega)|$ due to the vibrational mode for $\mathbf{M} = |\mathbf{M}|\hat{x}$ and $\mathbf{M} = |\mathbf{M}|\hat{y}$: (a) and (b) at $\mathbf{r}=(c, 0)=\mathbf{R}_0$; (c) and (d) at $\mathbf{r}=(-c, 0)$, demonstrating the filtering of the mirage signal.

what follows, we assume the coupling between the 2DEG and the VM to be weak.⁹

The QC enables signals to be transmitted between foci;¹³ it also provides a "cloak of invisibility", similar to what has been achieved with electromagnetic fields,¹⁷ where objects were made invisible within a certain frequency band. More specifically, the electronic properties of the QC govern the energy regime in which a signal transmitted from one focus can be observed at the other focus; in particular, signals within a certain frequency range can be hidden from observation.¹⁶ This cloaking can be seen in Fig. 5, where a density plot of the energy derivative of the LDOS $|\partial_\omega A(\mathbf{r}; \omega)|$ is shown — even when the VM is visible at the focus in which it is sitting (Fig. 5(a) and (b)), the QC cloaks it from observation at the other focus for Ω within a certain range (Fig. 5(c) and (d)).¹⁶ In this system, the ME effects allow the range over which cloaking occurs to be controlled by changing the orientation of \mathbf{M} — compare the results for $\mathbf{M} = |\mathbf{M}|\hat{x}$ and $\mathbf{M} = |\mathbf{M}|\hat{y}$. Said in another way, the ME effects allow one to filter the signal transmitted from one focus to the other.

Up to now, we have considered the system's electronic properties, assuming the QC's wall to be FM ordered. We have also considered the magnetic properties of the wall and, in particular, the wall's magnetic ordering tendencies;⁹ as the QC's wall is one-dimensional, fluctuations will suppress ordering, and an external field \mathbf{h} is necessary to stabilize the order. Fig. 6 shows results for the QC's magnetization for various values of \mathbf{h} . We see that the moments are disordered at zero field and, hence, the magnetization is zero; a nonzero magnetization is obtained as \mathbf{h} is increased. We have found that a FM aligned wall is obtained from readily accessible magnetic fields — $|\mathbf{h}| \simeq 0.2\pi(\rho_0 J)^2 E_F$; for reasonable values of the parameters, this gives $|\mathbf{h}| = \mathcal{O}(1 \text{ meV})$. [It is worth noting such values are considerably lower than Kondo tem-

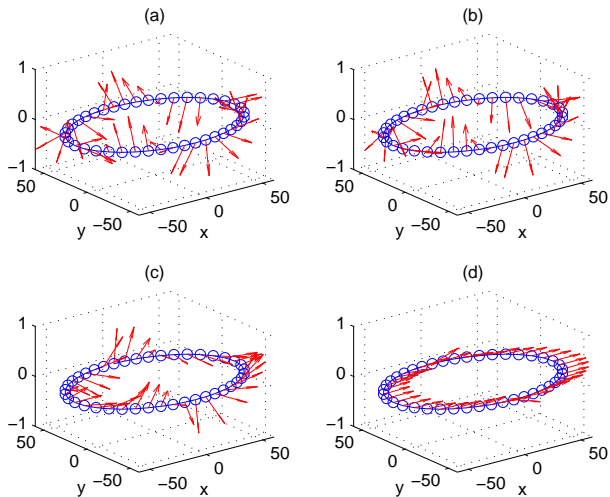


FIG. 6: Evolution of the magnetization with the external magnetic field \mathbf{h} : (a) $|\mathbf{h}|=0$ (b) $|\mathbf{h}|=0.04E_0$ (c) $|\mathbf{h}|=0.12E_0$ (d) $|\mathbf{h}|=0.24E_0$ where $E_0=\pi(\rho_0J)^2 E_F$.

peratures that have been observed from atoms/molecules on surfaces.^{18]} Furthermore, we have found the geometry can, in fact, be optimized, so that ferromagnetic ordering occurs at extremely small values of \mathbf{h} .

This work demonstrates proof of principle of the func-

tionality afforded by ME effects at the atomic scale; indeed, we were able to control the properties of systems placed inside the QC as well as their electronic signals/signatures. With a FM aligned wall, the ME effects allowed us to control the magnetic properties of atoms placed inside the QC, as well as to filter transmitted signals; different magnetization patterns for the wall,²⁰ as well as different QC geometries, could provide further flexibility and control. By placing several atoms/molecules inside the QC, one could engineer devices where the ME effects allow the entanglement¹⁹ between atoms/molecules to be manipulated. It should also be mentioned that the ME effects allow manipulation of the properties of the QC's wall — the QC's wall itself provides a unique magnetic system with interesting properties, which could also afford means of transmitting and manipulating information.^{21,22}

EHK acknowledges the warm hospitality of the Instituto de Física Teórica (Madrid, Spain), where most of this work was performed. SEU acknowledges support from AvH Stiftung, and the hospitality of the Dahlem Center for Complex Quantum Systems at FU-Berlin. This work was supported by NSF MWN/CIAM and PIRE grants (ATN and SEU), the Spanish Grants TOQATA and QUAGATUA (JRL), and the Spanish Grant FIS2009-11654 (JRL and EHK).

-
- ¹ W. Eerenstein, N. D. Mathur, and J. F. Scott, *Nature* **442**, 759 (2006); S.-W. Cheong and M. Mostovoy, *Nature Mat.* **6**, 13 (2007); R. Ramesh and N. A. Spaldin, *Nature Mat.* **6**, 21 (2007); and references therein.
 - ² M. N. Baibich, J. M. Broto, A. Fert, F. Nguyen Van Dau, F. Petroff, P. Eitenne, G. Creuzet, A. Friederich, and J. Chazelas, *Phys. Rev. Lett.* **61**, 2472 (1988).
 - ³ S. Jin, T. H. Tiefel, M. McCormack, R. A. Fastnacht, R. Ramesh, and L. H. Chen, *Science* **264**, 413 (1994).
 - ⁴ See, e.g. K. C. Nowack, F. H. L. Koppens, Yu. V. Nazarov, L. M. K. Vandersypen, *Science* **318**, 1430 (2007); C. Flindt, A. S. Sorensen, and K. Flensberg, *Phys. Rev. Lett.* **97**, 240501 (2006).
 - ⁵ E.M. Vogel, *Nature Nano* **2**, 25 (2007); N. Engheta, *Science* **317**, 1698 (2007); H. G. Craighead, *Science* **290**, 1532 (2000); and references therein.
 - ⁶ E. J. Heller, *Nature Physics* **4**, 443 (2008).
 - ⁷ G. Nicolay, F. Reinert, S. Hufner, and P. Blaha, *Phys. Rev. B* **65**, 033407 (2001); S. LaShell, B. A. McDougall, and E. Jensen, *Phys. Rev. Lett.* **77**, 3419 (1996).
 - ⁸ L. S. Rodberg and R. M. Thaler, *Introduction to the Quantum Theory of Scattering*, (Academic Press, New York, 1967).
 - ⁹ The Supplementary Information document provides details of our calculations and considerations.
 - ¹⁰ G. D. Mahan, *Many-Particle Physics*, 3rd ed. (Kluwer Academic/Plenum, New York, 2000).
 - ¹¹ A. C. Hewson, *The Kondo Problem to Heavy Fermions*, (Cambridge University Press, Cambridge, 1993).
 - ¹² J. D. Walls and E. J. Heller, *Nano. Lett.* **7**, 3377 (2007).
 - ¹³ H. C. Manoharan, C. P. Lutz, and D. M. Eigler, *Nature* (London) **403**, 512 (2000); C. R. Moon, C. P. Lutz, and H. C. Manoharan, *Nature Phys.* **4**, 454 (2008).
 - ¹⁴ E. Rossi and D. K. Morr, *Phys. Rev. Lett.* **97**, 236602 (2006).
 - ¹⁵ T. Holstein, *Ann. Phys. (San Diego, CA)*, **8**, 325 (1959).
 - ¹⁶ J. Fransson, H. C. Manoharan, and A. V. Balatsky, *Nano. Lett.* **10**, 1600 (2010).
 - ¹⁷ D. Schurig, J. J. Mock, B. J. Justice, S. A. Cummer, J. B. Pendry, A. F. Starr, D. R. Smith, *Science* **314**, 977 (2006).
 - ¹⁸ A. Zhao, Q. Li, L. Chen, H. Xiang, W. Wang, S. Pan, B. Wang, X. Xiao, J. Yang, J. G. Hou, and Q. Zhu, *Science* **309**, 1542 (2005); V. Iancu, A. Deshpande, and S.-W. Hla, *Phys. Rev. Lett.* **97**, 266603 (2006).
 - ¹⁹ L. Amico, R. Fazio, A. Osterloh, and V. Vedral, *Rev. Mod. Phys.* **80**, 517 (2008).
 - ²⁰ M. Bode, M. Heide, K. von Bergmann, P. Ferriani, S. Heinze, G. Bihlmayer, A. Kubetzka, O. Pietzsch, S. Blügel, and R. Wiesendanger, *Nature* (London) **447**, 190 (2007).
 - ²¹ C. F. Hirjibehedin, C. P. Lutz, and A. J. Heinrich, *Science* **312**, 1021 (2006).
 - ²² L. Zhou, J. Wiebe, S. Lounis, E. Vedmedenko, F. Meier, S. Blügel, P. H. Dederichs, and R. Wiesendanger, *Nature Phys.* **6**, 187 (2010).

Quantum manipulation via atomic-scale magnetoelectric effects: Supplementary Information

I. THE SYSTEM AND HAMILTONIAN

We consider a quantum corral made of magnetic atoms on a metallic surface with spin-orbit coupling (SOC). The Hamiltonian is $\hat{H}_{\text{QC}} = \hat{H}_0 + \hat{V}$, where \hat{H}_0 describes the two-dimensional electron gas (2DEG) of the surface, and \hat{V} describes the coupling of the 2DEG to the magnetic atoms. In second quantized form, the Hamiltonian for the 2DEG is

$$\hat{H}_0 = \int d\mathbf{r} \psi^\dagger(\mathbf{r}) \left[\frac{1}{2m} \mathbf{p}^2 + \lambda \hat{z} \cdot (\mathbf{p} \times \bar{\sigma}) \right] \psi(\mathbf{r}), \quad (7)$$

where $\psi^\dagger(\mathbf{r})$ is a two-component field operator for the 2DEG $\psi^\dagger(\mathbf{r}) = (\psi^\dagger_\uparrow(\mathbf{r}), \psi^\dagger_\downarrow(\mathbf{r}))$, and $\{\sigma^\mu\}$ are the Pauli matrices; the coupling of the 2DEG to the magnetic atoms is

$$\hat{V} = \sum_i \psi^\dagger(\mathbf{r}_i) \left(V_0 + \frac{J}{2} \bar{\tau}_i \cdot \bar{\sigma} \right) \psi(\mathbf{r}_i), \quad (8)$$

where $\bar{\tau}_i$ is the spin operator for the magnetic moment of the i^{th} atom, V_0 describes the potential scattering, and J is the exchange coupling between the 2DEG and the magnetic atoms. [As before, $\{\sigma^\mu\}$ are the Pauli matrices.]

As we are interested in the case where the wall is ferromagnetically ordered, we treat the magnetic moments of the atoms as classical variables; then $(J/2)\langle \bar{\tau}_i \rangle \rightarrow \mathbf{M}$. The quantity entering in the calculations is $(\pi\rho_0)|\mathbf{M}|$. To estimate this quantity, we consider, for concreteness, a spin-5/2 moment (which is relevant to e.g. Mn^{2+} atoms); we consider the physically reasonable value $\rho_0 J = 0.2$ — we obtain $(\pi\rho_0)|\mathbf{M}| \simeq 0.785$. Motivated by this value, in our calculations we used $(\pi\rho_0)|\mathbf{M}| = 0.5$. As noted in the text, however, our results are robust, as the corral's geometry can be tuned to enhance/optimize the magnetoelectric effects.

II. SCATTERING FORMALISM

The QC's GF can be written as

$$G(\mathbf{r}, \mathbf{r}'; \omega) = G_0(\mathbf{r}, \mathbf{r}'; \omega) + G_0(\mathbf{r}, \mathbf{R}_0; \omega) \hat{T}(\omega) G_0(\mathbf{R}_0, \mathbf{r}'; \omega). \quad (9)$$

In Eq. 9, the T -matrix $\hat{T}(\omega)$ describes the influence of \hat{H}_1 . Furthermore, $G_0(\mathbf{r}, \mathbf{r}'; \omega)$ is the bare GF of the QC — it is the GF in the absence of \hat{H}_1 ; it is determined by the Dyson equation

$$G_0(\mathbf{r}, \mathbf{r}'; \omega) = G_{00}(\mathbf{r}, \mathbf{r}'; \omega) + \sum_i G_{00}(\mathbf{r}, \mathbf{r}_i; \omega) (V_0 I + \mathbf{M} \cdot \bar{\sigma}) G_0(\mathbf{r}_i, \mathbf{r}'; \omega) \quad (10)$$

with $G_{00}(\mathbf{r}, \mathbf{r}'; \omega)$ being the free-particle GF i.e. the GF in the absence of the QC's wall (and also \hat{H}_1). $G_{00}(\mathbf{r}, \mathbf{r}'; \omega)$ is given by^{1,2} (for $\mathbf{r} \neq \mathbf{r}'$)

$$G_{00}(\mathbf{r}, \mathbf{r}'; \omega) = G_0^{00}(R; \omega) I + G_1^{00}(R; \omega) \begin{pmatrix} 0 & -i \exp(-i\theta) \\ i \exp(i\theta) & 0 \end{pmatrix} \quad (11)$$

where

$$G_0^{00}(R; \omega) = -i \frac{m}{4} \left\{ \left(1 + \frac{\lambda m}{k} \right) H_0[R(k + \lambda m)] + \left(1 - \frac{\lambda m}{k} \right) H_0[R(k - \lambda m)] \right\} \quad (12a)$$

$$G_1^{00}(R; \omega) = -\frac{m}{4} \left\{ \left(1 + \frac{\lambda m}{k} \right) H_1[R(k + \lambda m)] - \left(1 - \frac{\lambda m}{k} \right) H_1[R(k - \lambda m)] \right\} \quad (12b)$$

with $H_0(x) = J_0(x) + iN_0(x)$, $H_1(x) = J_1(x) + iN_1(x)$, and $\exp(i\theta) = [(x - x') + i(y - y')]/|\mathbf{r} - \mathbf{r}'|$. In the above equations, $J_0(x)$ and $J_1(x)$ ($N_0(x)$ and $N_1(x)$) are the Bessel function (Neumann function) of order-zero and order-1, respectively.³ Furthermore, $R = |\mathbf{r} - \mathbf{r}'|$ and k is such that $k^2/2m = \omega + (\lambda m)^2/2m$.

III. MAGNETIC IMPURITY

We consider a spin-1/2 magnetic impurity placed in the QC; the Hamiltonian is

$$\hat{H}_1 = J_K \bar{\tau} \cdot \psi^\dagger(\mathbf{R}_0) (\bar{\sigma}/2) \psi(\mathbf{R}_0) \quad (13)$$

where $\bar{\tau}$ is the impurity's spin operator. [$J_K > 0$.] To proceed, we treat $\bar{\tau}$ with a fermion representation — we write $\bar{\tau} = (1/2)f^\dagger \bar{\sigma} f$ where f^\dagger is the two-component spinor $f^\dagger = (f_\uparrow^\dagger, f_\downarrow^\dagger)$; the f -fermions satisfy the constraint $f^\dagger f = 1$. Then, Eq. 13 can be written as

$$\hat{H}_1 = -\frac{J_K}{2} (\psi^\dagger(\mathbf{R}_0) f) (f^\dagger \psi(\mathbf{R}_0)) . \quad (14)$$

As we are interested in the infrared fixed point of Eq. 13 (or, equivalently, Eq. 14), we employ mean-field theory⁴ — the infrared properties are determined by the effective Hamiltonian

$$\hat{H}_{\text{eff}} = \lambda f^\dagger f + \chi \psi^\dagger(\mathbf{R}_0) f + \chi f^\dagger \psi(\mathbf{R}_0) , \quad (15)$$

where χ and λ are (constants) determined self-consistently via

$$\frac{4}{J_K} \chi = -\langle \psi^\dagger(\mathbf{R}_0) f + f^\dagger \psi(\mathbf{R}_0) \rangle \quad , \quad \langle f^\dagger f \rangle = 1 \quad . \quad (16)$$

Then, the T -matrix in Eq. 9 is proportional to the f -fermions' retarded GF:⁴ $\hat{T}(\omega) = \chi^2 G^f(\omega)$, where

$$G^f(\omega) = -i\Theta(t) \langle \{f(t), f^\dagger\} \rangle(\omega) . \quad (17)$$

IV. VIBRATIONAL MODE

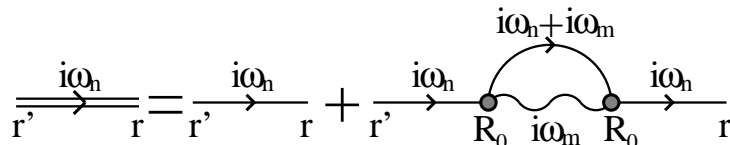


FIG. 7: QC's GF, taking into account the VM. The single solid (wavy) line denotes the QC's (VM's) bare GF.

Assuming the coupling between the VM and the 2DEG to be weak (i.e. g is small), we take the VM into account perturbatively. To lowest nontrivial order, the QC's GF (taking into account the VM) is given by the diagram in Fig. 7. Performing the Matsubara sum and analytically continuing to real frequencies, the T -matrix (in Eq. 9) is given by

$$\hat{T}(\omega) = g^2 \int \frac{d\nu}{2\pi} A_0(\nu) \left\{ \frac{[1 + n(\Omega) - f(\nu)]}{\omega - \nu - \Omega + i\delta} + \frac{[n(\Omega) + f(\nu)]}{\omega - \nu + \Omega + i\delta} \right\} , \quad (18)$$

where $A_0(\nu)$ is the corral's spectral function at the site \mathbf{R}_0 — $A_0(\nu)$ is such that the Matsubara GF can be written as⁵

$$G_0(\mathbf{R}_0, \mathbf{R}_0; i\omega_n) = \int \frac{d\nu}{2\pi} \frac{A_0(\nu)}{i\omega_n - \nu} .$$

V. MAGNETIC PROPERTIES OF THE QUANTUM CORRAL'S WALL

As we are interested in the magnetic properties of the QC's wall, we return to Eqs. 7 and 8 — we integrate out the 2DEG and obtain an effective spin Hamiltonian;⁶ the leading interaction generated⁷ is given by^{1,8}

$$\hat{H}_{\text{spin}} = -\frac{J^2}{4\pi} \sum_{i < j} \int d\omega f(\omega) \text{Im} \left\{ \text{Tr} [(\bar{\tau}_i \cdot \bar{\sigma}) G_0(\mathbf{r}_i, \mathbf{r}_j; \omega) (\bar{\tau}_j \cdot \bar{\sigma}) G_0(\mathbf{r}_j, \mathbf{r}_i; \omega)] \right\} , \quad (19)$$

where $f(\omega)$ is the Fermi function, and $G_0(\mathbf{r}_i, \mathbf{r}_j; \omega)$ is the retarded GF of the 2DEG in the absence of the exchange coupling J . To proceed efficiently, we employ a commonly used approximation, namely approximating $G_0(\mathbf{r}_i, \mathbf{r}_j; \omega)$ in Eq. 19 by $G_{00}(\mathbf{r}_i, \mathbf{r}_j; \omega)$.^{6,9} We have checked that *along the corral's wall*, $G_0(\mathbf{r}_i, \mathbf{r}_j; \omega)$ is similar to $G_{00}(\mathbf{r}_i, \mathbf{r}_j; \omega)$. [Of course this approximation fails inside the corral.] We obtain

$$\hat{H}_{\text{spin}} = \sum_{i < j} K_{ij} \bar{\tau}_i \cdot \bar{\tau}_j + D_{ij} \mathbf{Q}_{ij} \cdot (\bar{\tau}_i \times \bar{\tau}_j) + J_{ij}^0 (\mathbf{Q}_{ij} \cdot \bar{\tau}_i) (\mathbf{Q}_{ij} \cdot \bar{\tau}_j) , \quad (20)$$

where $\mathbf{Q}_{ij} = \hat{z} \times \hat{R}_{ij}$ with $\hat{R}_{ij} = (\mathbf{R}_i - \mathbf{R}_j) / |\mathbf{R}_i - \mathbf{R}_j|$ (\hat{z} is the unit vector perpendicular to the 2DEG), and the couplings are given by

$$\begin{aligned} K_{ij} &= -\frac{J^2}{2\pi} \int_0^{E_F} d\omega \text{Im} \left\{ [G_0^{00}(|\mathbf{r}_i - \mathbf{r}_j|; \omega)]^2 + [G_1^{00}(|\mathbf{r}_i - \mathbf{r}_j|; \omega)]^2 \right\} , \\ D_{ij} &= \frac{J^2}{\pi} \int_0^{E_F} d\omega \text{Re} \left\{ G_0^{00}(|\mathbf{r}_i - \mathbf{r}_j|; \omega) G_1^{00}(|\mathbf{r}_i - \mathbf{r}_j|; \omega) \right\} , \\ J_{ij}^0 &= \frac{J^2}{\pi} \int_0^{E_F} d\omega \text{Im} \left\{ [G_1^{00}(|\mathbf{r}_i - \mathbf{r}_j|; \omega)]^2 \right\} , \end{aligned}$$

where E_F is the Fermi energy. [$G_0^{00}(|\mathbf{r}_i - \mathbf{r}_j|; \omega)$ and $G_1^{00}(|\mathbf{r}_i - \mathbf{r}_j|; \omega)$ are given in Eqs. 12a and 12b.]

The magnetic properties of the QC's wall were determined by Monte Carlo simulations of Eq. 20 — the magnetic moments were treated as classical three-dimensional vectors of unit length; the minimum energy state of Eq. 20 was obtained via a simulated annealing procedure.

¹ H. Imamura, P. Bruno, and Y. Utsumi, Phys. Rev. B **69**, 121303(R) (2004).

² J. D. Walls and E. J. Heller, Nano Lett. **7**, 3377 (2007).

³ I. S. Gradshteyn and I. M. Ryzhik, *Table of Integrals, Series, and Products* (Academic Press, San Diego 1994).

⁴ A. C. Hewson, *The Kondo Problem to Heavy Fermions*, (Cambridge University Press, Cambridge, 1993).

⁵ G. D. Mahan, *Many Particle Physics*, (Kluwer Academic, New York 2000).

⁶ See e.g. K. H. Fischer and J. A. Hertz, *Spin Glasses* (Cambridge University Press, Cambridge, 1991).

⁷ This is the most relevant interaction generated in the renormalization group sense.

⁸ H.-H. Lai, W.-M. Huang, and H.-H. Lin, Phys. Rev. B **79**, 045315 (2009).

⁹ See, e.g. L. Brey et al, Phys. Rev. Lett. **99**, 116802 (2007); Q. Liu, C.-X. Liu, C. Xu, X.-L. Qi, and S.-C. Zhang, Phys. Rev. Lett. **102**, 156603 (2009); and references therein.